Proceedings of the 11th International Conference on Hydrodynamics (ICHD 2014)
October 19 – 24, 2014, Singapore

ADDED MASS AND DAMPING COEFFICIENTS FOR A UNIFORM FLEXIBLE BARGE USING VOF

J.H.KIM

Department of Naval Architecture and Ocean Engineering, Seoul National University
Gwanak-gu, Seoul, South Korea

P.A.LAKSHMYNARAYANANA, P.TEMAREL

Fluid Structure Interactions Group, University of Southampton
Southampton, Hampshire, United Kingdom

The main aim of this paper is the numerical investigation of the effect of domain size and mesh density on modeling the three-dimensional (3-D) the radiation problem using RANS CFD software. The solution for the radiation forces and moments, namely the added mass and damping coefficients, is obtained by imposing a simple harmonic oscillation to a marine structure floating in still water at the relevant mode shape. A uniform barge is used to illustrate the investigation, with the relevant symmetric mode shapes provided from the Euler beam theory. The hydrodynamic coefficients for symmetric oscillations of the barge are evaluated using an inviscid flow model in STAR-CCM+. These include the rigid body motions of heave and pitch and the 2- and 3-node distortion mode shapes. A range of mesh densities, between 1.1M and 9.6 M, are used to examine their effects with particular reference to low and high frequencies and the cross-coupling hydrodynamic coefficients between rigid and distortion modes. The influence of the damping zone on the solution is also examined. The RANS CFD predictions are compared with the results from a three-dimensional potential flow boundary element method, allowing for hull distortions.

1. Introduction

Substantial progress has been made during the last few years in dealing with the nonlinear response of a rigid ship travelling in regular waves, using potential flow analysis and Reynolds Averaged Navier-Stokes (RANS) methods [1]. Prediction of the nonlinear behaviour of a flexible hull in waves using 3-D flow analysis, on the other hand, has not received much attention. Dealing with hydroelasticity is of vital importance considering the increasing size ships and offshore structures, as rigid body assumptions to evaluate the wave-induced motions and loads of real ships will, inherently, omit important dynamic features [2, 3]. Use of RANS method, either through commercially available or in-house software, has been relatively widespread in modelling violent flows associated with, for example, slamming and sloshing [4, 5]. However, their application to model the problems of seakeeping and wave-induced loads has been relatively limited. For example, there are applications for the two-dimensional radiation problem of obtaining the hydrodynamic coefficients in sway, heave and roll [6] and the 3-D problem presented by Paik et al. involving CFD and FEM codes and different ways of coupling [7].

In this paper we present the computations of hydrodynamic coefficients of a stationary uniform rectangular barge, in still water, undergoing forced simple harmonic oscillations in symmetric rigid body and distortion modes, for a range of frequencies between 0.2 and 2.0 rad/s. These computations were carried out using the STAR-CCM+ software, using the inviscid flow option, and 3-D modelling. The predictions were compared against three-dimensional potential flow results using the Green's function for pulsating source. The eigen vectors for the distortion modes were calculated using polynomial approximations fitting the Euler beam idealisation. The main aim of this paper is to highlight the effects of domain size, mesh density and the influence of damping zone on the predicted hydrodynamic coefficients, in the range of frequencies investigated. Particular attention is paid to the cross coupling coefficients and satisfaction of relevant symmetry conditions.

2. Numerical Modelling

2.1. *The Numerical Method*

The RANS equations form the mathematical background of the methodology in the STAR-CCM+ software used in this paper [8]. For the case of inviscid flow these reduce to the well-known Euler equations. In this software a finite volume method is used to discretize the fluid domain with control volumes (CVs) corresponding to the size of computational cells. The integral form of conservation equations is discretized and applied to each cell centre. Each equation is a function of pressure and velocity at the cell centre and in the neighbouring cells. FOR nonlinear equations iterative techniques are applied for linearization. The mid-point method is used to compute the space integrals, implying that the surface integrals are a product of the integrand at the cell face centre and the area of the face and the volume integrals are the product of mean integrand value and the CV. Both are 2^{nd} order accurate if the integrand is also calculated to 2^{nd} order accuracy. The Hybrid Gauss-Least Square gradient method is used to solve the transport equations.

2.2. *The Numerical Model of the Barge*

The geometry under consideration is a uniform rectangular barge, whose main particulars are given in Table 1. Both the geometry and fluid domain were modelled using the inbuilt CAD modelling option in STAR-CCM+ which provides various volume meshing models [8]. In this study, a combination of trimmer and extruder mesh was used. Trimmer cell mesher is a robust and efficient method of producing high quality hexahedral meshing with minimal cell skewness. Once a core mesh is identified and generated, extruder mesher produces orthogonal extruded cells for specific boundaries. Based on the extrusion parameters (i.e. number of layers, stretching ratio, extrusion magnitude) the mesh is extruded from the specific boundary in normal direction. Extruder meshing not only aids in saving the global cell count of the model but also assists in efficiently refining the cells in regions where the flow features have to be accurately captured. The mesh growth rate was kept under 1.1 to prevent any wave reflections arising due to sudden change in mesh sizes of adjacent cells.

Table 1. Main particulars of the Rectangular Barge.

Main Particulars	Barge
Length	120 m
Breadth	7 m
Depth	11.15 m
Draft	5.575 m

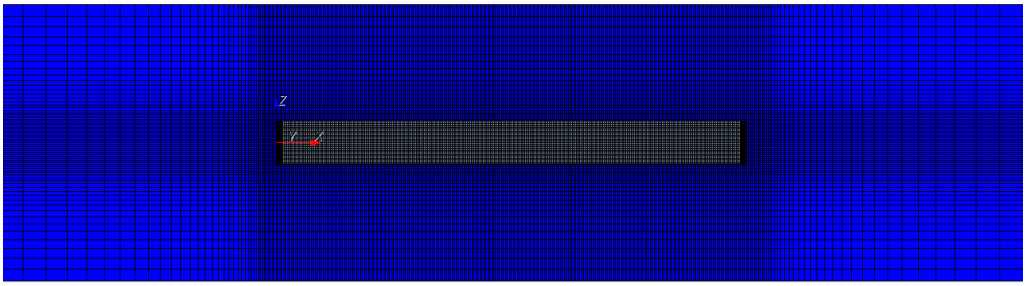

Figure 1. Core mesh of barge (xz plane) and the extrusion of inlet and outlet

The domain is modelled in three dimensions, with x along the barge and y and z in athwarthships and vertical directions, respectively. The generated core mesh (xz plane) for a particular case, corresponding to 2.6 million cells, is shown in Figure 1. The size of the domain was decided based on the wave lengths of individual frequencies. The length of the inlet, outlet and the domain breadth were

divided into two zones, namely wave propagation zone and the damping zone. The lengths of both these zones were equal to the wavelength of the radiated wave. The Star-CCM+ inbuilt volume of fluid damping (VOF) option, introducing resistance to the vertical motion, was activated in the damping zone. The water and air depth (z direction) was 0.5*wavelength for deep water condition. The range of frequencies investigated was from 0.2 rad/s to 2.0 rad/s in steps of 0.2 rad/s, as illustrated in Table 2 with their respective domain sizes. Additional meshes used are discussed in Section 4.

Table 2. Summary of frequencies investigated and their respective domain sizes.

Frequency	0.2 rad/s	0.4 rad/s	0.6rad/s	0.8 to 2.0 rad/s
Wavelength	1539.658 m	384.914 m	246.345 m	61.583 m
Wave Propagation Zone	1539.658 m	384.914 m	246.345 m	61.583 m
Damping Zone	1539.658 m	384.914 m	246.345 m	61.583 m
Water & Air Depth	769.829 m	192.457 m	123.1725 m	30.79 m
Number of Cells	4.4 million	2.6 million	2.2 million	1.1 million

2.3. *Boundary Conditions, Motions and Solution*

The boundary conditions were selected so that they mimic the conditions of a towing tank. Since the body used in this study is symmetrical about its longitudinal axis, symmetry plane boundary condition was used and only one half of the rectangular barge was modeled. STAR-CCM+ provides various options to assign motion to a body. Morphing motion was used in this study to assign motion to the barge. Morphing is a dynamic mesh technique where the points and their associated displacements are interpolated by the morpher throughout the region to displace the actual vertices of the discretized domain. Deformation of morpher control points was specified using grid velocities. The regions and their respective boundary conditions and morpher motion is summarized in Table 3.

Table 3. Regions and their corresponding boundary conditions morpher motion and damping

Region Name	Boundary Condition	Morpher Motion	Damping Condition
barge (body)	wall	Grid velocity	
inlet	wall	fixed	VOF damping
outlet	wall	fixed	VOF damping
sym_wall	symmetry plane	NA	
top	wall	fixed	
bottom	wall	fixed	
wall (y extent)	wall	fixed	VOF damping

The velocity of a body undergoing simple harmonic motion is given by:

$$\dot{y} = \omega y_a \cos \omega t \qquad (1)$$

where $\dot{y}$ is the velocity, ω is the frequency of oscillation (rad/s), y_a the amplitude and t time (s). Morphing motion is imposed using grid velocities computed using Equation (1). In this study we are interested in the rigid body motions of heave and pitch and the vertical 2- (2VB) and 3- node (3VB) distortions. The grid velocity for each morphing motion was imposed as a vector multiplying the velocity in Equation (1) with the eigen vector for individual rigid body motions or distortions. For example the grid velocity vector for heave is:

$$gridvelocity = \omega y_a \cos \omega t * eigenvector \qquad (2)$$

where [0, 0, 1] is the eigen vector for heave.

The eigen vectors for the distortion modes were calculated using Euler Beam theory approximated using polynomials. VOF wave model was used to initialise the air-water interface. That is to say a first order wave with zero amplitude was initialised to model the still water condition. The inviscid computations were performed with the help of an implicit unsteady solver and 2nd order discretization scheme. For numerical stability, local Courant numbers given by $CFL = U\Delta t / \Delta x$, should in general be less than 1. CFL relates to the cell dimension Δx, time step Δt and the flow velocity U. The time step for each simulation was calculated ensuring the Courant number is approximately 0.4. The phase velocity of the radiated wave was used as the flow velocity U. The excitation amplitude was 1 m for frequencies less than 1 rad/s and 0.2m for frequencies equal to or greater than 1 rad/s.

2.4. *Hydrodynamic Coefficients of the Barge*

To obtain the added mass and damping coefficients of the barge undergoing oscillations given by Equation (1), the dynamic force component in the direction of motion is required. In morphing motion the body is considered massless, i.e. at static condition the vertical force on the body is the initial buoyancy. The dynamic force is the difference of the static force from the total force experienced by the barge. Static and total forces for rigid body motion and distortions were successfully calculated in STAR-CCM+ with user-defined field functions. The static force on the body was calculated on the mean free surface. The vertical dynamic force distribution along the barge was then transformed into a generalised force F_{rs}(t), by multiplying with the s^{th} eigenvector and integrating along the barge [3]. Here r denotes the index of the mode at which the barge is oscillated. Instantaneous values of the hydrodynamic coefficient are obtained by Fourier analysis of the dynamic force F_{rs}(t) time history using discrete windows approach for one period, $T=2\pi/\omega$, of oscillation, namely

$$A_{rs} = \frac{2}{T\omega^2} \int_{t-T/2}^{t+T/2} F_{rs}(\mathrm{t}) \sin(\omega t) dt \tag{3}$$

$$B_{rs} = -\frac{2}{T\omega} \int_{t-T/2}^{t+T/2} F_{rs}(\mathrm{t}) \cos(\omega t) dt \ . \tag{4}$$

3. Results and Discussion

The results of a stationary uniform barge harmonically oscillating, at the relevant mode shapes, at a free surface are presented in this section. Predictions using inviscid flow with STAR-CCM+ for the diagonal and off-diagonal terms were compared against three-dimensional potential flow results using the pulsating source Green's function [3]. Good agreement was seen in the diagonal terms but discrepancies were noted in the off-diagonal terms, especially in relatively low frequencies.

To investigate these discrepancies (a) extended domain and (b) refined grids. The size of the extended domain was based on a wavelength corresponding to the frequency of 0.1 rad/s and had a total cell count of about 6.8 million. In this case the refinement on the body and free surfaces was similar to other, coarse, meshes used (see Table 2). As it is not practical to eliminate reflected waves, and their effects on the predictions at lower frequencies, the extended domain was used to run computations in cases where the predictions deviated largely from the 3-D potential flow results. For refined grids, for the sake of simplicity, a refinement ratio (fine mesh size/coarse mesh size) of 2 is used around the body in the core mesh and the adjacent cell size in the extruder mesh is maintained as 1.1 for all directions. The refinement ratio on the free surface was a little more than √(2). Use of refinement resulted in an increase in the total grid size by a factor of about 4. For example, in the case of 0.4 rad/s the refined grid has a total cell count of 9.6 million.

The hydrodynamic coefficients calculated for the rigid body motions of heave and pitch are presented in Figure 2. A very good agreement with potential theory predictions can be observed. A sudden slump is seen at ω=1.6 rad/s in the hydrodynamic coefficients calculated using potential theory in all cases,

corresponding to an irregular frequency. In the case of pitch the discrepancies noted at 0.4 and 0.8 rad/s in Figures 2(c) and (d), respectively, were further investigated. Use of the extended (6.8M) mesh did not change the predictions significantly. However, use of the refined grids (fine) resulted in closer agreement with potential flow results.

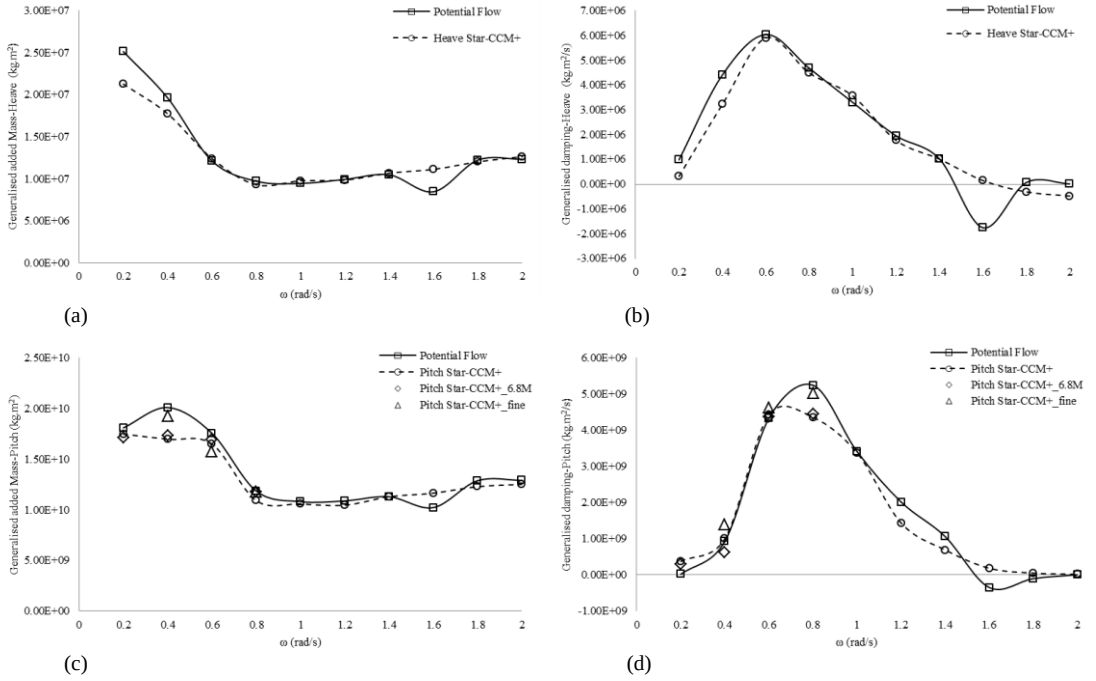

Figure 2. Comparison between generalized added mass and damping coefficients obtained from 3-D potential flow analysis and CFD analysis (inviscid): (a) & (b) Heave motion, (c) & (d) Pitch motion

The comparisons of hydrodynamic coefficients for the distortion modes are shown in Figure 3. The agreement with potential flow results is better for the added mass than the fluid damping coefficients. Differences in fluid damping were observed in the lower frequencies and the numerical results showed slight over prediction when compared to potential flow results. Further investigations were carried out for the 3VB hydrodynamic coefficients with additional meshes for 0.4 to 0.8 rad/s. Neither an improvement nor any deterioration was seen in the predictions using the extended domain (6.8M). In the case of refined grids (fine), slightly better agreement was observed compared to the potential flow.

The predictions for cross-coupling coefficients between Heave and 2-node (2VB) distortion mode and Pitch and 3-node (3VB) distortion are presented in Figures 4 and 5, respectively. It is expected that the upper diagonal and lower diagonal terms will be same for a stationary symmetrical body, such as the barge use in this study.

The off-diagonal terms of Heave-2VB and 2VB-Heave compare well with potential flow results, except for significant differences observed at low frequencies. Computations using the extended domain (6.8M) show some improvement for the added mass at 0.2 rad/s, but no improvement for the damping. The calculated off-diagonal terms improved using the refined grid (fine) at 0.4 rad/s. Although a small difference is observed when compared to potential flow, the CFD-predicted cross-coupling damping coefficients are close to each other.

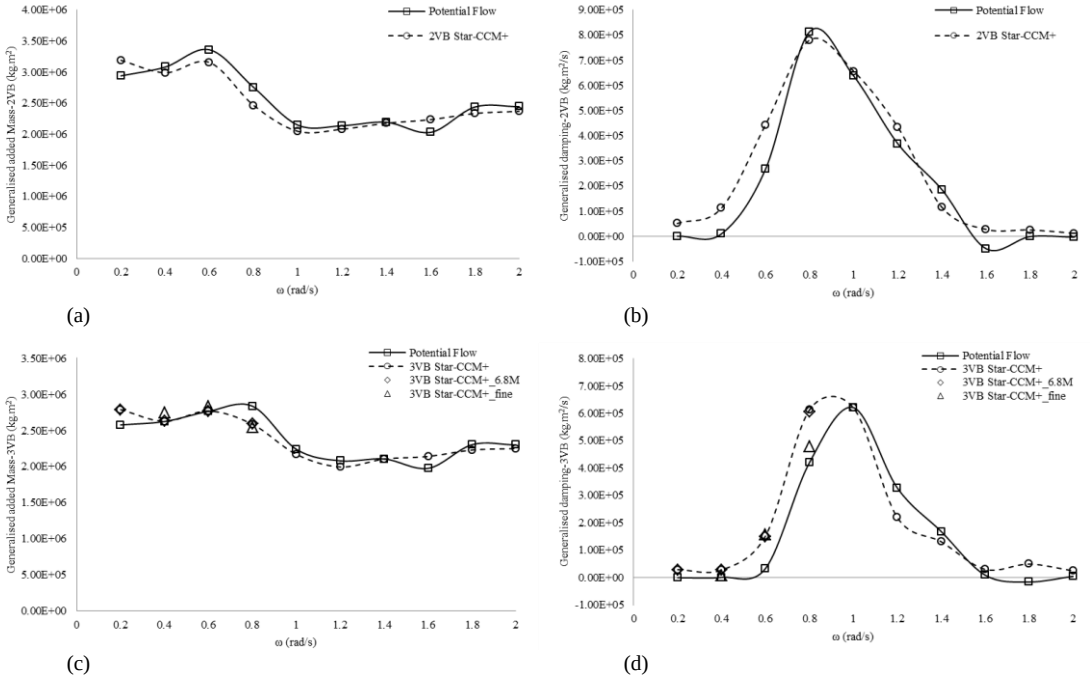

Figure 3. Comparison between generalized added mass and damping coefficients obtained from 3-D potential flow analysis and CFD analysis (inviscid) : (a) & (b) 2-node distortion mode, (c) & (d) 3-node distortion mode

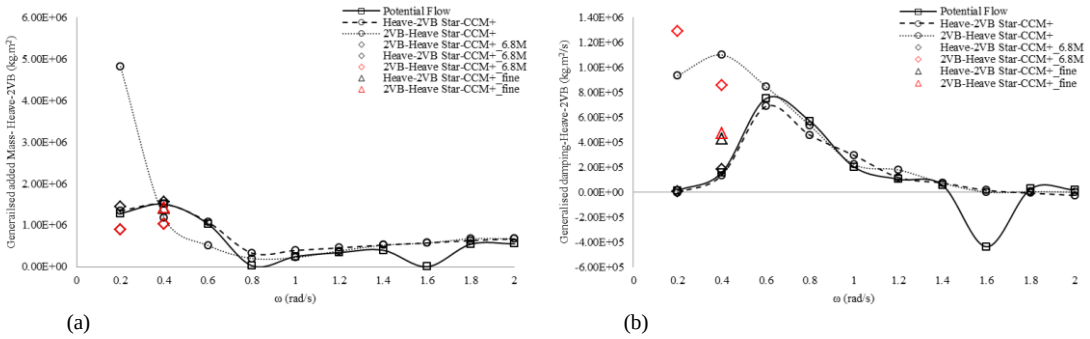

Figure 4. Comparison between generalized added mass and damping cross coupling coefficients obtained from 3-D potential flow analysis and CFD analysis : (a) & (b) coupling coefficients of Heave in 2-node distortion and 2-node distortion in Heave.

CFD predictions presented for Pitch-3VB and 3VB-Pitch terms show least agreement with potential flow results. Except for a few frequencies Pitch-3VB shows better agreement than 3VB-Pitch coefficients. Furthermore, the CFD predictions show large deviations when compared with each other. Omitting the relatively lower frequencies, added mass coefficients showed better symmetry than the damping coefficients which showed large deviations for all frequencies investigated.

As observed in the previous cases, use of extended fluid domain model (6.8M), by and large, made only small improvements to the agreement of inviscid CFD predictions with potential flow, and no improvement to the symmetry relationships. There is a substantial improvement in the predicted coefficients when using the refine grids (fine). The asymmetry in the magnitude of the off-diagonal coefficients is much less for the refined grids. Differences in the level of agreement with potential flow can be partially explained by the fact that although the computations are done using an inviscid model, CFD solves Navier-Stokes equations which account for non-linearity.

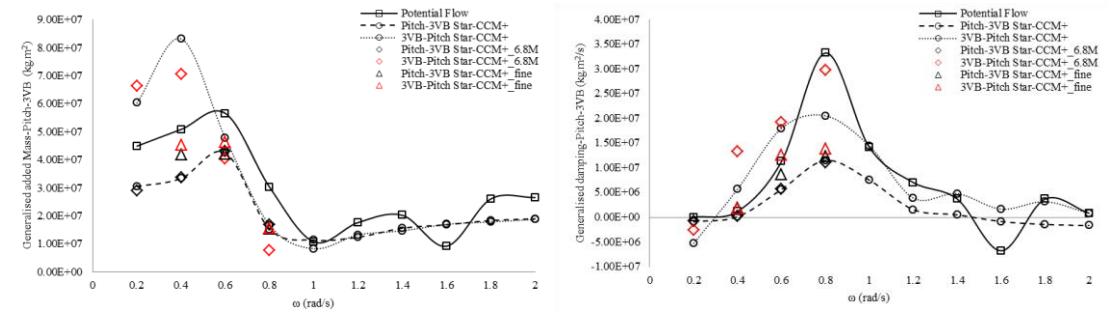

(a) (b)

Figure 5. Comparison between generalized added mass and damping cross coupling coefficients obtained from 3-D potential flow analysis and CFD analysis : (a) & (b) coupling coefficients of pitch in 3-node distortion and 3-node distortion in pitch.

The difference in the calculated coefficients for the 3VB-Pitch term for the refined grids is highest among all mesh densities, compared to the Pitch-3VB term. This could be attributed to the complexity involved in calculating the generalized forces in the 3-node distortional mode when compared to the rigid body motion. The magnitude of dynamic forces are quite small in relatively lower frequencies and the accuracy in calculating the forces is very sensitive to the mesh refinement on the body. The mesh refinement on the free surface also contributes largely to the radiated wave pattern and flow field, and thus the hydrodynamic coefficients.

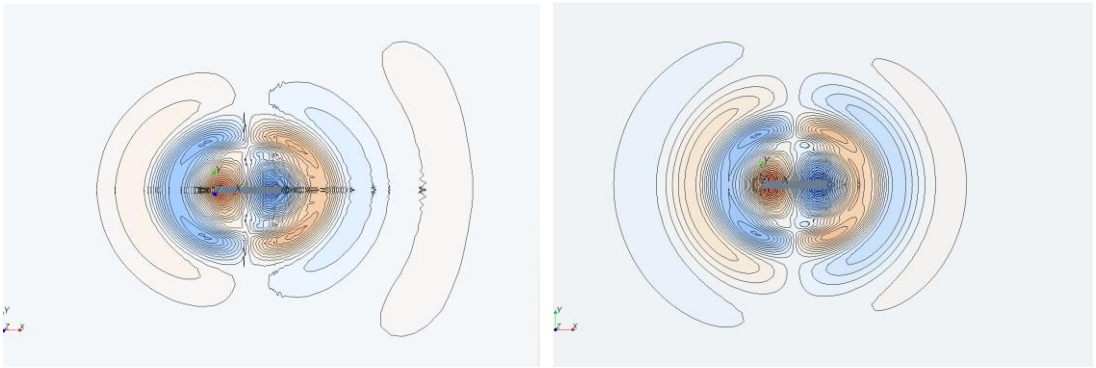

(a) (b)

Figure 6. Contour lines of radiated waves for pitch mode at 0.8 rad/s taken at t=10.0s : (a) extended domain; (b) refined grid.

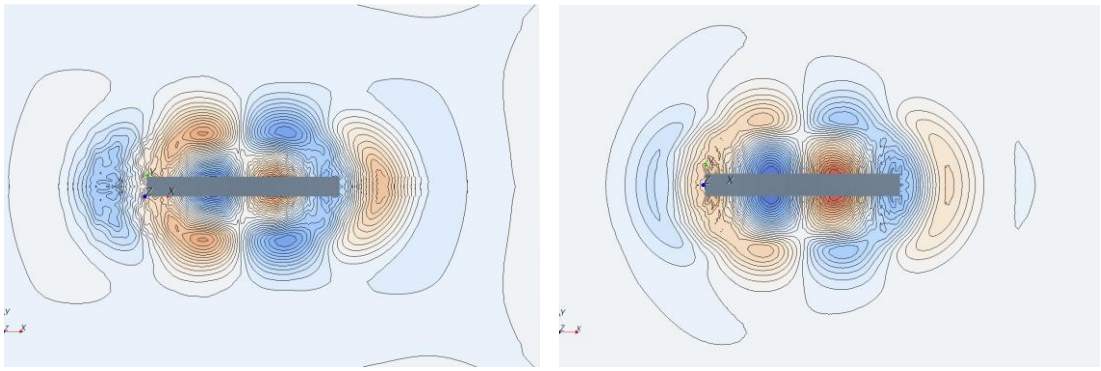

(a) (b)

Figure 7. Contour lines of radiated waves for 3VB mode at 0.8 rad/s taken at t=10.0s : (a) extended domain; (b) refined grid.

Figure 6 and 7 show the contour lines of the waves radiated away from the body for the extended domain (6.8M) and refined grid. The wave contours in the pitch motion, shown in Figure 6, are not significantly different from each other for either model. Except for a few numerical noises in the far

field, the radiated waves for the rigid body motion do not change much for the refined grid as compared to the coarse mesh of the extended domain. However differences can be spotted in the case of the 3-node distortional mode, shown in Figure 7. The waves radiated from the body dampen out very close to the body in the coarser mesh of the extended domain, whereas, in the refine grid there is less numerical noise around the body, and better defined wave crests and troughs are developed. Along with the symmetry in the calculated coefficients, the flow field contours also contribute in predicting the hydrodynamic coefficients with a good degree of accuracy.

4. Conclusions

In this work, hydrodynamic coefficients of a stationary barge harmonically oscillating in still water was successfully calculated using STAR-CCM+, with inviscid flow option, for symmetric rigid body and distortional modes, and compared to results from a 3-D potential flow method. Good agreement was achieved in most cases investigated, with some exceptions for the cross-coupling coefficients. Computations in lower frequencies were particularly difficult due to the large length of the radiated wave which calls for large domains and damping zones to prevent any wave reflections. The discrete time window for the calculation of hydrodynamic coefficients is also large in the case of low frequencies, which is likely to introduce errors in calculations. The dynamic force in the low frequencies is very small when compared to the static component; hence the results are very sensitive to mesh densities. Extended domain and damping zones did not improve the quality of solution in relatively lower frequencies. Major discrepancies were observed in the case of cross coupling between 3VB and Pitch modes which can be eliminated to a large extent using refined grids. It is concluded that by comparing the symmetry in the cross-coupling coefficients and observing the radiated wave contour, the radiation problem of a symmetric body can be solved with confidence and accuracy.

The next stage of the investigation will involve the coupled antisymmetric (horizontal bending and twisting) hydrodynamic coefficients, likely to introduce further complexities in terms of radiated waves.

Although this investigation was limited to the radiation problem, namely added mass and damping coefficients, the conclusions drawn are applicable to the modelling of the behaviour of ship in regular waves, a problem currently being investigated.

Acknowledgements

The authors from University of Southampton would like to gratefully acknowledge the support from Lloyd's Register and the Lloyd's Register Foundation through its University Technology Centre.

References

1. ISSC, Report of Committee I.2: Loads. **1** 79–150 (2012).
2. Bishop, R.E.D. and Price, W.G., *Hydroelasticiy of Ships*, Cambridge University Press (1979).
3. Bishop, R.E.D., Price, W.G. and Wu, Y., A general linear hydroelasticity theory of floating structures moving in a seaway. *Phil. Trans. R. Soc. Lond.* **A316** 375–426 (1986).
4. Brizzolara, S., Couty, N., Hermundstad, O., Kukkanen, T., Ioan, A., Kukkanen, T., Viviani, M. and Temarel, P., Comparison of experimental and numerical loads on an impacting bow section. *Ships and Offshore Structures* **3(4)** 305-324 (2008).
5. Brizzolara, S., Savio, L., Viviani, M., Chen, Y.G., Temarel, P., Couty, N., Hoflack, S., Diebold, L., Moirod, N. and Souto Iglesias, A., Comparison of experimental and numerical sloshing loads in partially filled tanks. *Ships and Offshore Structures* **6(1-2)** 15-43 (2011).
6. Querard, A.B.G., Temarel, P. and Turnock, S.R., Application of RANS to hydrodynamics of bilge keels and baffles. *William Froude Conference on Advances in theoretical and applied hydrodynamics* – Past and Future, Portsmouth, GB (2010).
7. Paik, K.J., Carrica. P.M., Lee, D. and Maki, K., Strongly coupled fluid–structure interaction method for structural loads on surface ships. *Ocean Engng* **36** 1346–1357 (2009).
8. STAR-CCM+, STAR-CCM+ version 7 manual. (2012).